



Society of Petroleum Engineers

SPE-191814-18ERM-MS

A New Algorithm for Processing Distributed Temperature Sensing DTS

Timothy Carr and Payam Kavousi Ghahfarokhi, West Virginia University; BJ Carney and Jay Hewit, Northeast Natural Energy, LLC; Robert Vagnetti, National Energy Technology Laboratory, US Department of Energy

Copyright 2018, Society of Petroleum Engineers

This paper was prepared for presentation at the SPE Eastern Regional Meeting held in Pittsburgh, Pennsylvania, USA, 7 - 11 October 2018.

This paper was selected for presentation by an SPE program committee following review of information contained in an abstract submitted by the author(s). Contents of the paper have not been reviewed by the Society of Petroleum Engineers and are subject to correction by the author(s). The material does not necessarily reflect any position of the Society of Petroleum Engineers, its officers, or members. Electronic reproduction, distribution, or storage of any part of this paper without the written consent of the Society of Petroleum Engineers is prohibited. Permission to reproduce in print is restricted to an abstract of not more than 300 words; illustrations may not be copied. The abstract must contain conspicuous acknowledgment of SPE copyright.

Abstract

Distributed temperature sensing (DTS) was used to record temperature from early 2016 to present for a Marcellus Shale horizontal dry gas well, MIP-3H, located in Monongalia County, West Virginia. In addition, after wellbore clean-out with water and nitrogen a flow scanner production log was conveyed on March 02, 2017. The flow scanner provides one day of gas and water production from each of the 28 stages in MIP-3H and from each of the clusters. The DTS data provides an opportunity to inspect the reservoir for Joule-Thompson (JT) effect, a phenomenon that describes cooling of a non-ideal gas as it expands from high pressure to low pressure, and obtain a relative production attribute along the lateral of the MIP-3H. The original fiber-optic DTS data shows the temperature along the lateral; however, due to the geometry of the well with toe up and the presence of a small fault and minor water production at Stage 10 relative gas production of each stage cannot be directly determined from the raw DTS data. We present two methods to generate DTS attributes that can be used to better reveal relative gas and water production through time from each perforation cluster and each stage of the MIP-3H. The first attribute deals with the deviations of the DTS measurements from the calculated geothermal temperature, while the second attribute calculated the difference between DTS temperature and the average daily DTS temperature along the lateral of the MIP-3H. We show that the latter DTS attribute provides a more robust image of temperature variations regime along the lateral than the former attribute. Negative values of the DTS attributes reveals JT cooling, resulting from stages of the MIP-3H with higher natural gas production. A correlation analysis of the production log with the calculated DTS attributes suggests that the production log is not representative of the entire production life of MIP-3H well. Temporal correlation with the DTS attributes is highest close to the production log recording day (March 2, 2017) decrease rapidly and the weak correlation switches from positive to negative.

Introduction

Background

The multidisciplinary and multi-institutional team of the Marcellus Shale Energy and Environmental Laboratory (MSEEL) works on geoscience, engineering, and environmental research in collaboration with

Northeast Natural Energy LLC, several industrial partners, and the National Energy Technology Laboratory of the US Department of Energy. The MIP-3H well is located in the core play area of the Marcellus Shale, in Monongalia County, West Virginia. The lateral of the MIP-3H landed and stayed in the target zone just above the Cherry Valley Limestone in the Marcellus Shale (Figure 1).

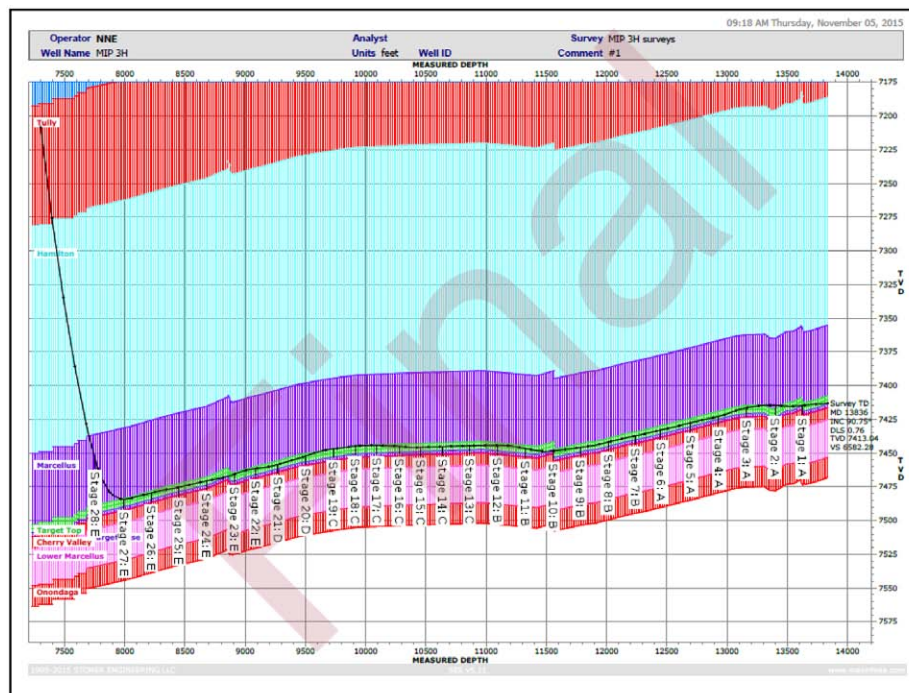


Figure 1—The MIP-3H well trajectory. Due to the geometry of the formation the toe of the well is approximately 60ft TVD (18m) structurally higher than the heel of the well.

The MIP-3H stimulation over 28 stages involved injection at high pressure, averaging 8500 psi (58.6 MPa), to fracture the formation and establish a complex network of propped permeable fracture pathways. A permanent fiber-optic cable was attached along the outer part of the casing to record acoustic vibrations during completion. Distributed acoustic sensing (DAS) provides a measure of relative strain and injection energy. Distributed temperature sensing (DTS) was also recorded during stimulation and at intervals of several times per day during the subsequent production period.

Each stage is approximately 200 feet (60m) long and has 4 to 5 perforation clusters, each consisting of 4-5 shots/foot. The spacing between stages varies between 20 to 50 feet (6-15m) with an average of 24 feet (7m) between plug depths to the nearest cluster in the previous stage. Clusters within each stage are spaced at 30-50 feet (9-15m) intervals. The MIP-3H well is a dry gas well, and after initial production and outside of the clean-up associated with the production logging, produces less than 10 barrels of water per day. Daily gas and produced water production is updated monthly and is available on the MSEEL website (<http://www.mseel.org>).

Analysis of microseismic, core and log data coupled with with DAS and DTS fiber-optic monitoring during completion in the Marcellus Shale shows the influence and interaction of both the present stress regime and the preexisting healed and calcite cemented small faults and numerous clusters of fractures oriented approximately east-west (Carr et al. 2017; Kavousi et al. 2017). Many of these preexisting factures led to uneven stimulation between clusters, and where faults and fractures are relatively more concentrated, allowed DAS attributes to detect communication of stimulation fluids between stages (Kavousi et al. 2018).

This study deals with the DTS data recorded during a production interval from May 5, 2016 to May 1, 2018. The two years of DTS data along with a flow scanner log on March 2, 2017 provides the opportunity to monitor production behavior with time.

DTS Basics

DTS technology utilizes a fiber-optic cable to measure temperature around the cable. A fiber-optic cable is composed of a core, which is the light carrying element, and cladding, which provides the lower refractive index for total internal light reflection throughout the cable (Nath et al., 2005, 2006). A fiberoptic system sends laser pulses at 10-ns or less down the length of the optical fiber. Incident lights collide with the molecular and lattice structure of the fiber medium and photons get scattered from the fiber-medium. The majority of photons that collide with the atoms in the fiber-medium are elastically scattered and have the same frequency and wavelength as the incident light. This energy preserved scattering, which is the strongest signal, is called a Rayleigh scattering. Brillouin scattering is an inelastic scattering that takes place when acoustic waves vibrate the fiber lattice at the molecular level and change the local refractive index of the optical fiber. In addition, a part of incident photons are scattered through the inelastic Raman Effect, in which the energy of the scattered photon might be higher or lower than the incident photon (Brown, 2006). The scattered photon could gain energy from displacing the fiber molecules to a lower vibrational energy state (anti-Stokes scattering), or lose energy to the fiber-medium molecules and raise them to a higher vibrational energy state (Stokes scattering). The energy of a photon is inversely proportional to its wavelength: higher energy anti-Stokes scattered photons have shorter wavelength than lower energy Stokes scattering. The intensity of the anti-Stokes scattering is strongly dependent on the temperature, while the longer wavelength Stokes signal is less temperature dependent. The ratio of these intensities is directly proportional to the temperature of the optical fiber at the point where backscattering takes place. In a DTS system, backscattered lights are filtered to remove the Rayleigh and Brillouin backscatters, to evaluate the intensity ratio of Stokes and anti-Stokes Raman waves. The velocity of light in the optical fiber is usually less than the speed of light and can be calculated as:

$$v = \frac{c}{n} \quad \text{Eq. 1}$$

Where c is the speed of the light and n is the fiber refractive index, which is usually between 1.5 and 1.7 (Smolen and van der Spek, 2003). Thus, a 10-ns long laser will correspond to approximately a 2 meter segment of the fiber, with a refractive index of 1.5. This will turn the optical fiber into a multi-point temperature sensor in the subsurface. This superiority over single point temperature measurement gauges has made the DTS a widely used and efficient temperature measurement tool.

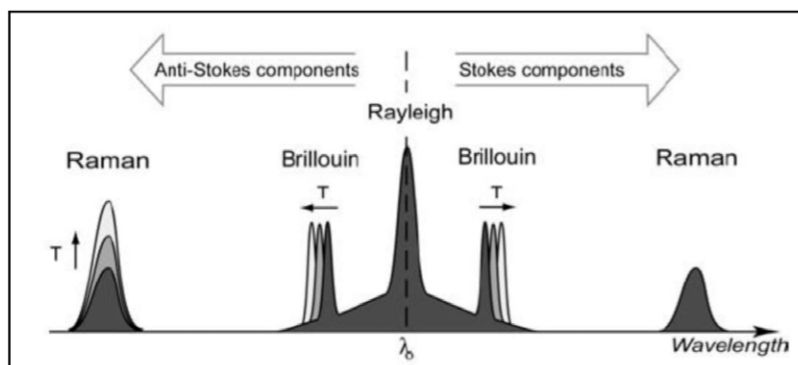


Figure 2—The incident laser is backscattered in different wavelength Raman and Brillouin waves; however, a majority of the incident laser is backscattered with the same wavelength as the incident laser through Rayleigh scattering. An increase in temperature (T) results in movement of the Brillouin waves and an increase in the Anti-Stokes components of Raman waves (Courtesy of Mishra et al., 2017).

Application of DTS

Various industries using temperature change in DTS systems as an indication of abnormal behavior or an imminent failure of a system such as a pipeline, pressure vessel, fire detection in tunnels, etc. (Peck and Seebacher, 2000; Barber et al., 1999; Walker and Carr, 2003; Mishra et al., 2017). The oil and gas industry has used DTS technology in various places around the globe for different field development applications. Companies have used DTS to monitor steam flood enhanced oil recovery operations in a downhole environment where temperature exceeds 400 degrees Fahrenheit (Karaman et al., 1996; Gonzales et al., 2018; Carnahan et al., 1999). DTS has also been used to infer production profiles from horizontal and vertical wells (Lanier and Adams, 2003; Tolan et al., 2001; Wang 2012; Nath et al., 2007; Saputelli et al., 1999; Ouyang and Belanger, 2006; Kabir et al., 2008; Johnson et al., 2006). DTS can provide valuable information about the geothermal gradient if used as a well log. Liquid or gas production can affect the DTS readings and provide information about the point of entries for hydrocarbons. Gas production in horizontal wells is associated with a drop in pressure and change in volume, which is therefore accompanied by a change in temperature. The Joule-Thompson effect describes the temperature change for a real gas or liquid when it is forced through a porous plug (throttling) in an adiabatic process (Roy 2002). This temperature variation is governed by the Joule- Thompson coefficient (JTC or μ_{JT}) as:

$$\mu_{JT} = \left(\frac{\partial T}{\partial P}\right)_h \quad \text{Eq.2}$$

where T is Temperature, P is pressure and h is specific enthalpy (Cengel and Boles, 2008). The equation shows the rate of change of temperature versus pressure, at constant enthalpy. During a sudden pressure drop, the sign of the μ_{JT} describes the temperature change as:

$\mu_{JT} < 0$, temperature increase

$\mu_{JT} = 0$, temperature remains constant

$\mu_{JT} > 0$, temperature decreases.

Pinto et al. (2012) undertook a linear mixing approach to predict μ_{JT} for a natural gas, which has methane as the major component, at various pressures and temperatures. Natural gas showed a positive μ_{JT} for pressure ranges from 72.5psi to 3625.9psi at temperatures of -9.4°F , 35.6°F , 80.6°F , and 170.6°F . The temperature usually decreases when gas enters the wellbore and increases when oil or water enters the wellbore (Brown et al., 2006). Brown et al., (2006) carried out DTS data analysis for a horizontal well in offshore peninsular Malaysia, in the South China Sea, to diagnose the oil production drop. They showed that a gas cap expansion, detected by a temperature drop through DTS, limited liquid production from the reservoir. Wang et al., (2008) proposed a flow-profiling model using DTS data for oil and gas wells. They showed, through analytical and numerical modeling, that the Joule-Thompson (JT) effect usually happens in gas wells except in very high bottom hole pressures around 8000psi where a warming effect might occur. Tight gas reservoirs, such as Marcellus Shale, have considerable pressure draw-downs close to the horizontal wellbore and so the JT effect should be observed. The cooling effect for gas can vary between 2 to $>20^\circ\text{F}$ per 1000psi pressure drawdown; in contrast, water produces a warming effect of around $3^\circ\text{F}/1000\text{psi}$ (Johnson et al., 2006).

DTS can also reveal cross-stage flow communication in unconventional oil and gas reservoirs during hydraulic fracturing (Ghahfarokhi et al., 2018; Amini et al., 2017). Leakage through plugs during hydraulic fracturing was also observed as abnormal DTS measurements during stimulation of a horizontal well in the Eagle Ford Shale (Wheaton et al., 2016).

We evaluated two years of DTS data during production from the MIP-3H well in the Marcellus Shale to reveal temperature variations during time that could be related to Joule-Thompson effect.

Discussion and Results

The DTS data from May 2016 to May 2018 along the horizontal section of the MIP-3H was compiled in a matrix with 950,000 measurements and was visualized in a waterfall plot (Figure 3). The DTS temperature shows that the toe of the well is relatively cooler than the heel of the well. Moreover, local cooler perforations can be observed from 9,500 to 10,500ft. However, the raw DTS data appears to be dominated by high temperature bands that are persistent along the well, especially during days with high production. Note that the MIP 3H supplies the City of Morgantown and along with the other three MIP wells is directly tied to seasonal and even daily variations in consumption due changes in demand due primarily to weather.

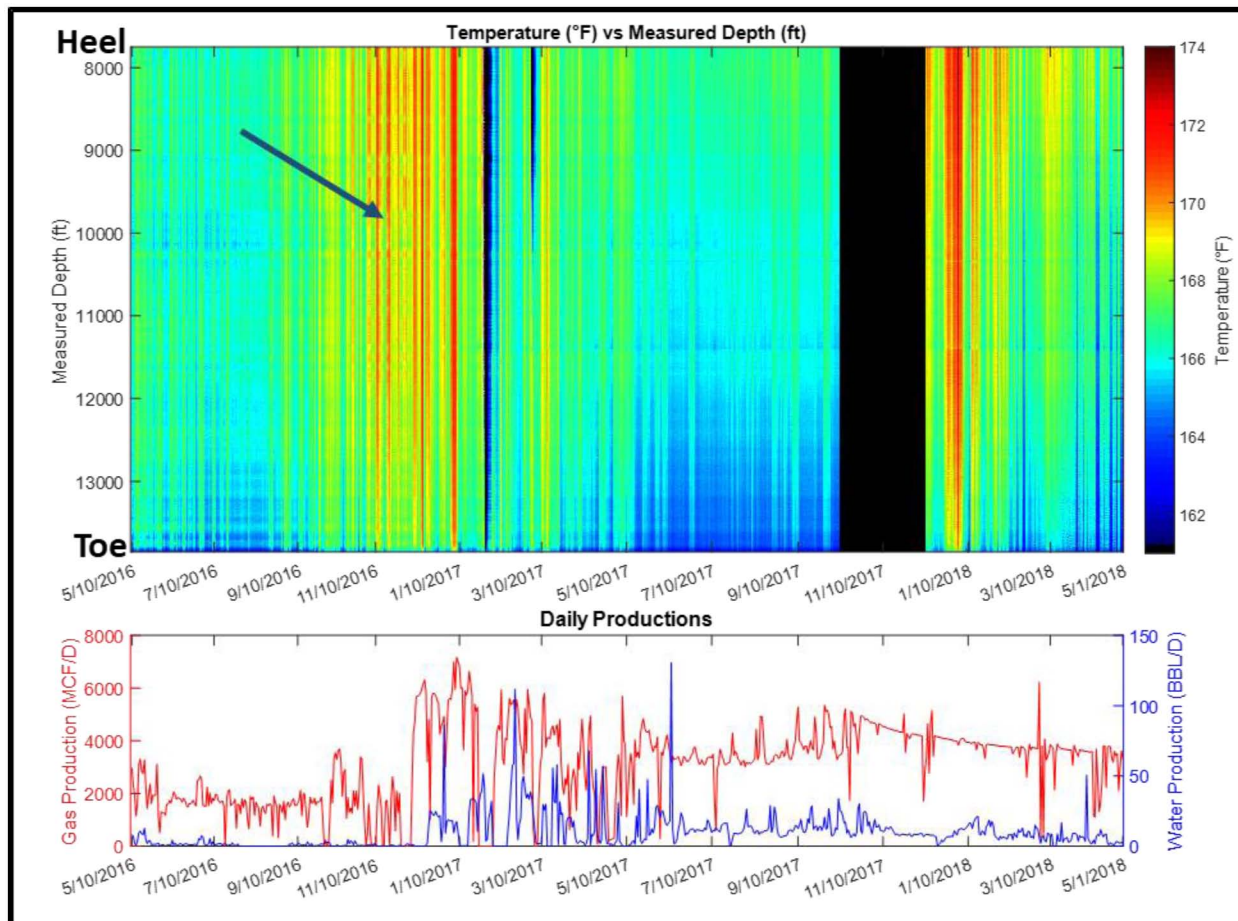


Figure 3—Upper plot shows the measured DTS from May 2016 to May 2018 from the heel (lower measured depth) to the toe (greater measured depth) of the lateral MIP-3H displayed as a waterfall plot. Gas and water production is shown in the lower graph. The large black section corresponds to missing data as a result of equipment issues. The arrow shows one of the high temperature bands during a period of high gas production.

The average daily temperature from the DTS data along the lateral follows the gas production trend from the well (Figure 4). The MIP-3H well is nearly horizontal, the elevation difference between toe and heel is approximately 60 feet (18m) TVD. This elevation difference is considered in this study to ensure an accurate estimation of geothermal temperature.

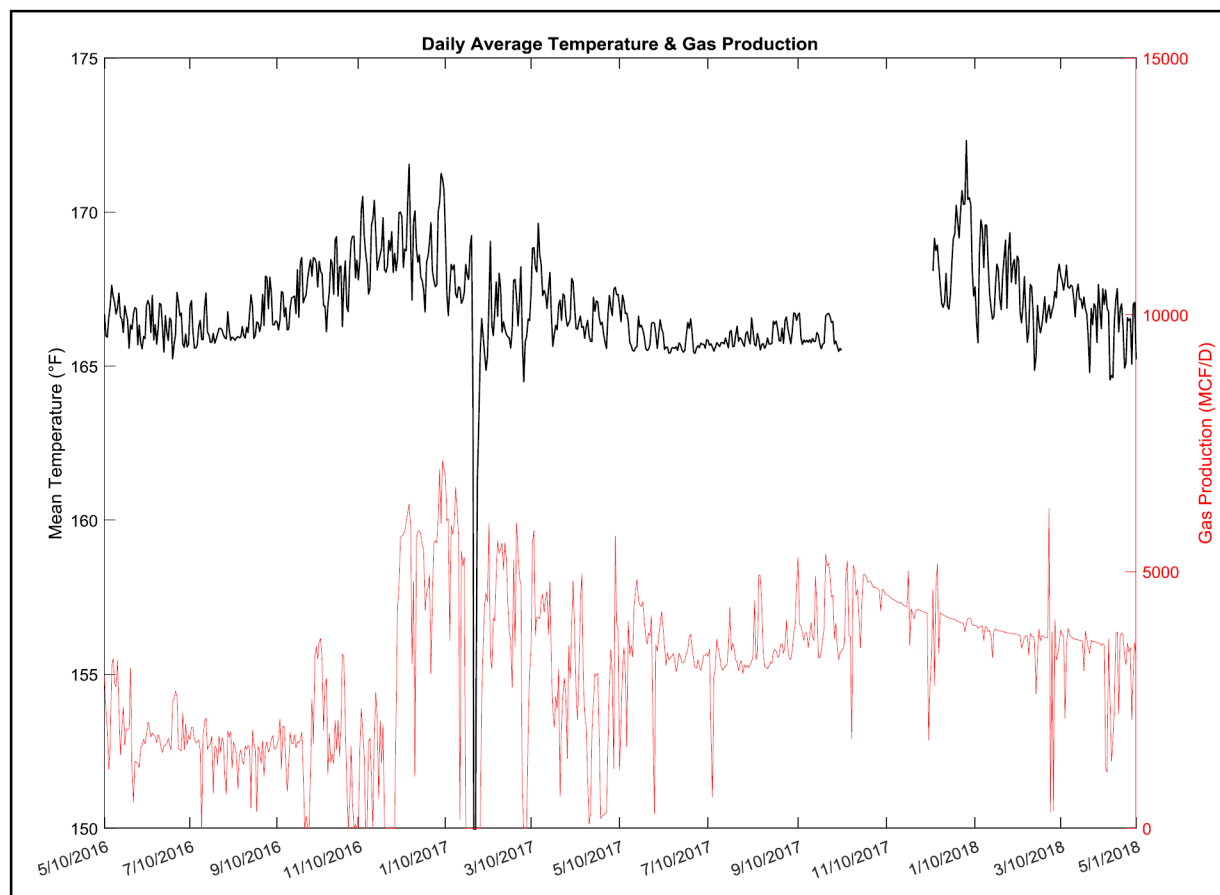


Figure 4—Average daily DTS temperature along the well is shown with gas production for the entire dataset. Note that DTS was not available for several months in late 2017.

We undertook two approaches to evaluate the Joule-Thompson (JT) effect for the MIP-3H. First, a conventional approach of temperature deviation from the geothermal temperature was assessed for JT effect. A 158°F bottom hole temperature (BHT) from well logging and an annual mean surface temperature of 52°F yielded a geothermal gradient of 1.35°F/100ft. BHT values are usually underestimated because of cooling effect of circulating mud in wells prior to logging. Deighton et al., (2014) suggested that BHT might be underestimated by 5-10°C (up to 30°C in some basins) due to varying heat conductivity of overlying formations. Frone et al., (2015) assessed the geothermal gradient for the Appalachian basin in West Virginia. They noted that BHT data from deeper than 1,000 meters is usually underestimated because of drilling fluid circulation. An equation was suggested to correct the BHT measurements between 1 Km (3280.84ft) and 3.9 Km (12795.27ft) as:

$$\Delta T = -16.51 + 0.018z - 2.34 \times 10^{-6}z^2 \quad \text{Eq. 3}$$

where z is the depth in meters, and T is the temperature in Celsius (Frone et al., 2015). The vertical pilot well for the MIP-3H recorded a BHT of 158°F at a depth of 7,834 feet, during well logging operations. Applying Equation 3 results in a BHT of 172°F that corresponds to a geothermal gradient of 1.53°F/100ft, which falls within the expected range of 25° to 30° C/km (1.36° to 1.64°F/100ft; Fridleifsson et al., 2008). This gradient was utilized to evaluate the JT cooling effect for the MIP-3H. Because the MIP-3H trajectory is almost horizontal, Figure 5 has a very similar trend to the measured temperatures in Figure 3. However, the well has more cooling toward the toe and more warming toward the heel. Geothermal temperature can be predicted using the geothermal gradient and the trajectory of the well. Then, we subtracted the predicted geothermal temperature from the DTS measured temperature profile in Figure 3. A negative deviation

from the geothermal temperature might suggest gas production (Figure 5). However, this temperature deviation attribute has uncertainties associated with variations in production of water along the lateral, the geothermal gradient, annual mean surface temperature, BHT measurement, and the assumption that layers above the Marcellus Shale are horizontal. A thermal-coupled fluid flow simulation such as Wang (2012) might shed light on reservoir properties. However, such a model will be a stochastic model due to uncertainties associated with geothermal gradient and reservoir properties.

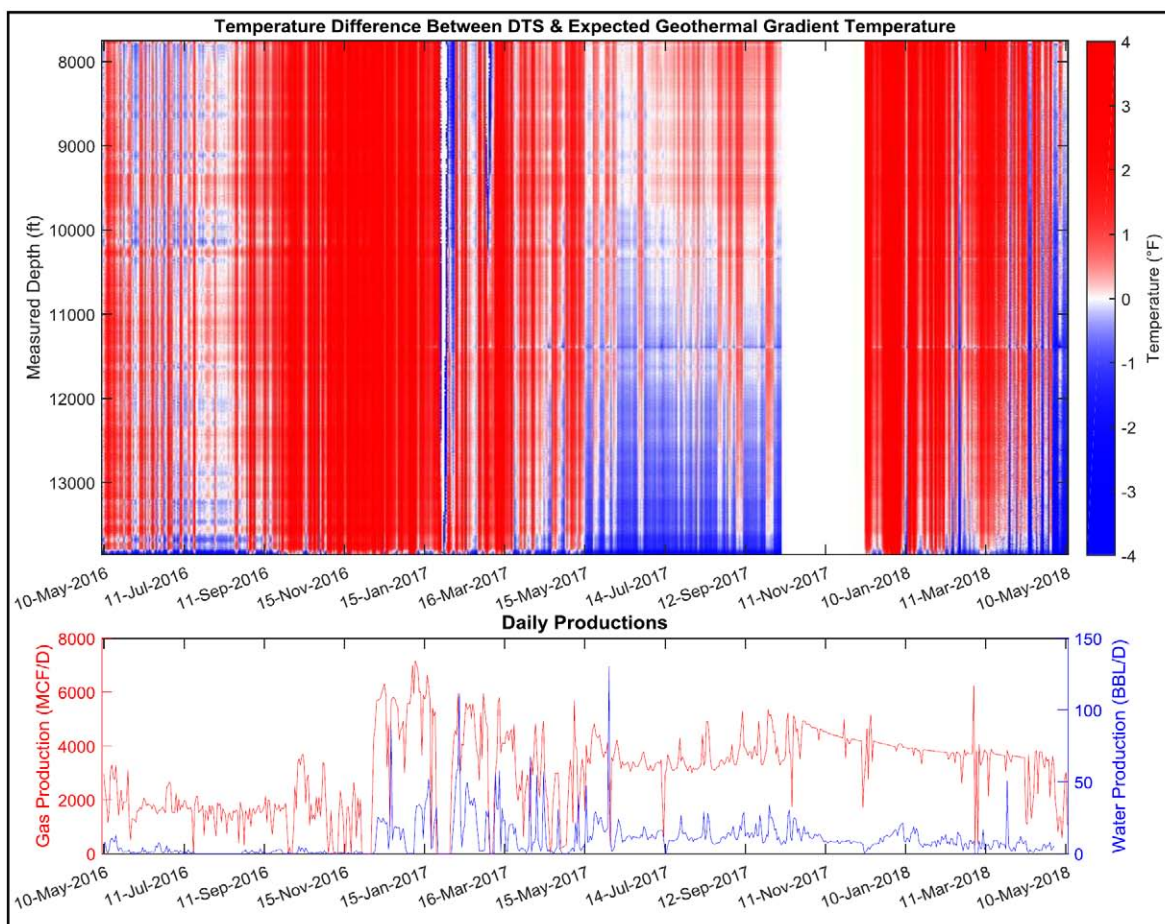


Figure 5—The difference each day between DTS measurements and calculated geothermal temperature is shown along the lateral of the well from the heel to the toe. Although dominated by vertical positive deviations due to changes in production, note the horizontal streaks that define individual perforations.

In another approach, we removed the trend of the DTS data introduced by the daily gas production. The average daily DTS temperature along the lateral is not a constant number and varies directly with the production rate from the well (Figure 4). Thus, DTS temperature deviations from the daily average temperature of the lateral were calculated. The de-trended DTS data also shows that cooling is more prevalent closer to the toe than the heel (Figure 6). In comparison to Figure 5, which shows temperature deviations from the expected geothermal temperature, the second approach provides a smoother image of the subsurface temperature variation. Moreover, it is independent from the variations in seasonal and daily gas production, geothermal gradient, surface temperature, and overlying stratigraphy.

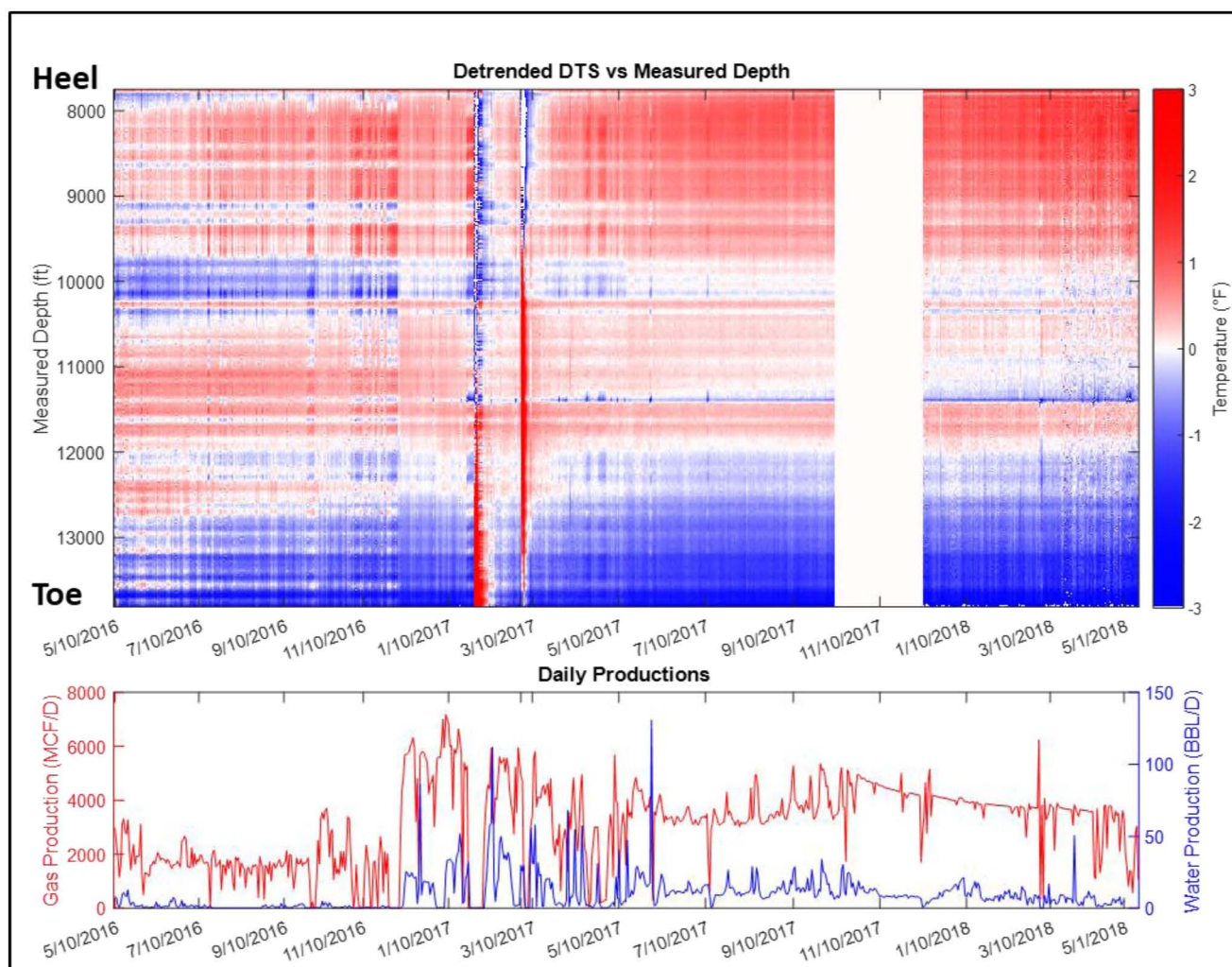


Figure 6—The de-trended DTS measurements show cooling close to the toe than the heel. Note that perforations are better defined in the de-trended DTS than DTS deviation attribute in Figure 5.

The de-trended DTS attribute can be upscaled to the stages scale (28 stages) to illustrate temperature variations for each stage relative to daily average temperature of each stage along the well (Figure 7).

On the production de-trended DTS attribute, general cooling from the heel to the toe is still observable, but some stages such as 10 and 11 and 20-21 and 23-28 are relatively warmer. Also standing out are the cooler stages 17-19. By integration of image logs, DAS and DTS data, and DAS attributes, a fracture swarm and small fault were observed in Stage 10 that resulted in a non-optimum stimulation and communication with the previous stages (Carr et al. 2007; Amini et al. 2007 and Ghahfarokhi et al. 2018). MIP-3H also has a production log (PLT) that was recorded on March 2, 2017. The production log from the MIP 3H shows the interpreted entry of produced water at stage 10 and flow downward toward the heel (Figure 8). While temperature usually decreases when gas enters the wellbore and the entry of fluid in this case the entry of water will result in an increase in temperature (Brown et al., 2006). This increase in relative temperature has persisted through the entire production interval sampled. Many of the stages that were engineered with selective positioning of clusters (stages 13-19) show relative cooling. While stages 23-28 near the heel show increases in the relative temperature attribute. These stages at the lowest part of the well may be affected by pooling of relative warmer water, and the toe stages producing more gas relative to the heel stages (figures 7 and 8).

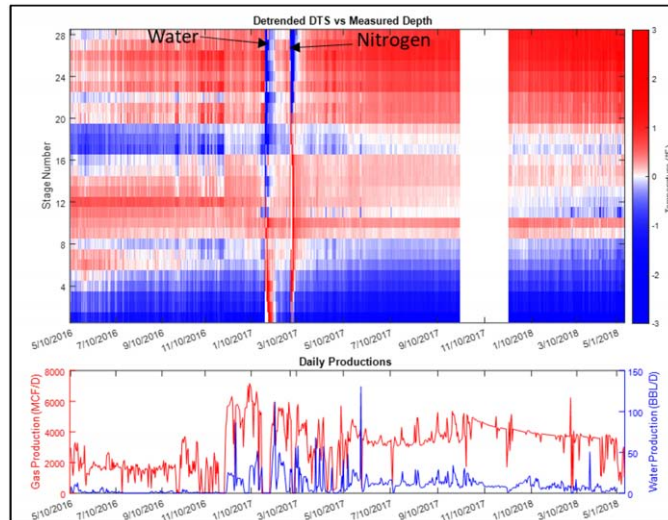


Figure 7—The de-trended DTS attribute is averaged to the stage scale. The arrows show the time that MIP-3H was washed with water and then with nitrogen foam prior to production logging.

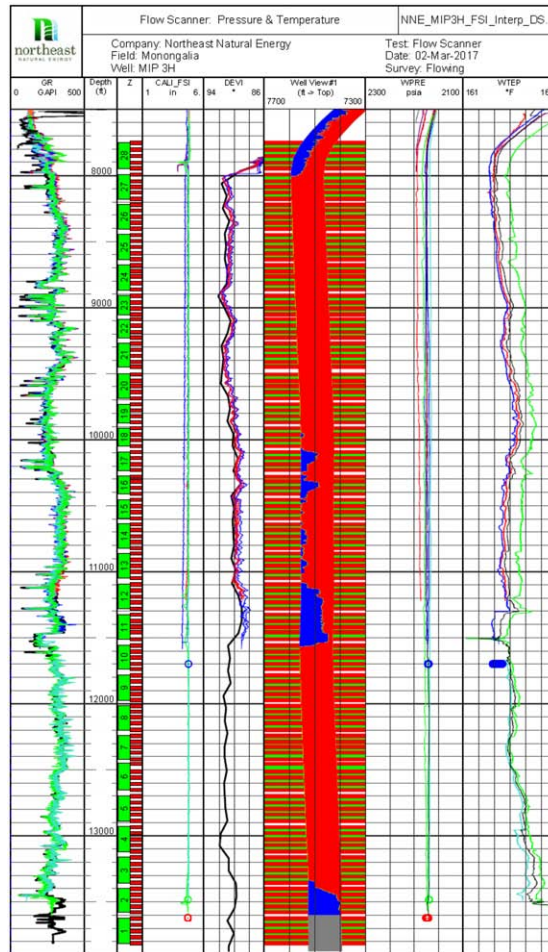


Figure 8—Production log for the MIP 3H showing 4 individual attempts, only one of which reached to near the toe of the lateral. Deepest log data was recorded at 13,530 ft. MD. The deviation track (Track 5) shows that on average the MIP 3H heel is deeper than the toe, but that relatively low spots exist from stages 4 to 10 and 23 to 27. The Wellview track (Track 6) shows the measured gas holdup (red) and water holdup (blue) directly related to trajectory; water (heavy phase) collects in low spots (deviation < 90 degrees) and immediately after Stage 10 while gas (light phase) collects on the high-side. The entry of water at Stage 10 results in a change in the temperature curves (Track 8). It is believed that water entry at stage 10 is related to fracture swarms and a small fault and flows toward the heel.

The de-trended DTS data shows that clusters underwent changes after washing the well with water and later by nitrogen foam. The gas production rate is significantly increased in late 2016 (almost 3 times that of previous trend). As reservoir pressure depletes, gas volume expands in the reservoir. Consequently, a higher gas rate within the fractures is expected, which increases the drag force around the proppants. That might mobilize proppants and pinch out some portion of the fractures. This could damage near wellbore conductivity and hence lowers the gas production later during the life of the reservoir. The washing procedures affected the temperature variations just for a limited time. The major factor appears to be the gas rate from the reservoir that resulted in lower gas productivity in some perforations. Recent DTS data from 2018 suggests that an unconstrained stabilized production is causing a general cooling effect for the entire well but is more pronounced close to the toe, water is being produced at Stage 10, and that water is increasing to collect in the relative low area near the heel.

Stage 10 in Figure consistently shows warming during the length of this study. This stage was previously studied by several researchers and has been shown to have several pre-existing faults and around 160 identified fractures. Ghahfarokhi et al., (2018) showed evidence of these faults and fractures reactivations from microseismic and distributed acoustic sensing (DAS) data. We suggest that high concentration of faults and fractures contributed to an ineffective hydraulic stimulation, and subsequent higher water production.

We calculated the correlation coefficients between each perforation's production from the PLT and the two temperature deviation attributes proposed in this study (Figure 9). The de-trended DTS shows a higher correlation with the PLT especially on the day of production logging. The correlation coefficients decrease rapidly away from this event and turns from positive to negative correlations. This could be due to our observations that stages close to the toe are getting colder and stages close to the heel are getting warmer. Production logging was carried out after washing with water and nitrogen, as shown in Figure 7. Washing the well significantly changed the downhole temperature and created temporal temperature anomaly in days close to the production logging. The poor correlation between the PLT log and the rest of the DTS data could cast doubt on the one day PLT results directly representing the earlier and later life of the reservoir. However, the PLT log provides critical insight into using the DTS to interpret gas and water production along the lateral and among stages.

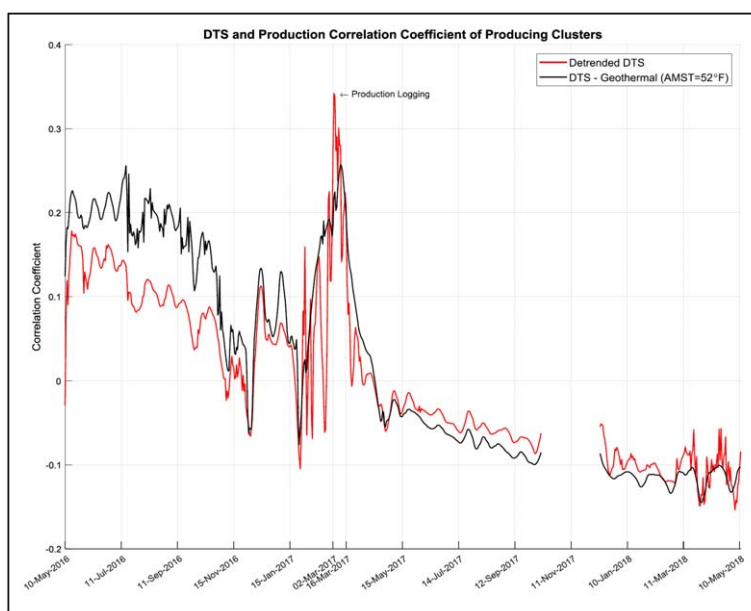


Figure 9—The correlation coefficients between two DTS attributes and the production log are presented. The de-trended DTS shows relative higher correlation with the production log than the DTS geothermal deviation attribute at and after the production logging event. All correlation coefficients are relatively small. Note the reversal in correlation coefficient sign from positive to the negative before and after the production logging event.

Conclusions

Two DTS temperature attributes are presented in this paper. Both attributes suggest that cooling is more dominant closer to the toe of the MIP-3H but varies by stage and through the production history. The decrease of DTS temperature attribute across the toe and engineered stages (stages 13-19) is suggestive of the Joule-Thompson cooling effect as a result of relatively higher gas production. The increased DTS temperature attribute at Stage 10 and near the heel is suggestive of water production and may affect gas production. We show that the DTS geothermal deviation attribute is affected by the geothermal gradient of overlying formations. This brings uncertainties to interpreting the resulted DTS deviation attribute. A second approach was presented that de-trends the daily DTS data by removing variations in daily gas production for the entire lateral. This de-trended DTS attribute is independent from the temperature gradient of the overlying formations and changes in production.

We showed that the correlation between production logging measurements and DTS attributes is highest on the production logging day and decreases rapidly and changes its sign from positive to negative. We suggest that the de-trended DTS attributes, when integrated with other petrophysical and geophysical data and tied to a single one day production log is a valuable attribute that can provide a temporal and spatial perspective to better understand relative production in the subsurface.

Acknowledgements

This research is funded through the U.S.DOE National Energy Technology Lab part of their Marcellus Shale Energy and Environmental Laboratory (MSEEL) (DOE Award No.: DE-FE0024297). We appreciate Northeast Natural Energy LLC. for providing data and technical support. Schlumberger is to be complimented for providing good robust data in the face of multiple technical challenges.

References

1. Amini, S., Kavousi, P. and Carr, T.R., 2017. Application of Fiber-optic Temperature Data Analysis in Hydraulic Fracturing Evaluation--A Case Study in Marcellus Shale: Unconventional Resources Technology Conference (URTEC), doi: [10.15530/URTEC-2017-2686732vb](https://doi.org/10.15530/URTEC-2017-2686732vb)
2. Barber, K., Jansen, M., Nokes, G. and Gatland, R., 1999, Fibre optic monitoring takes the heat off cables: *Modern Power Systems*, **19**(12), pp.35–37.
3. Brown, G.A., 2006, Monitoring Multilayered Reservoir Pressures and GOR Changes Over Time Using Permanently Installed Distributed Temperature Measurements: In SPE Annual Technical Conference and Exhibition. *Society of Petroleum Engineers*, SPE 101886. doi: [10.2118/101886-MS](https://doi.org/10.2118/101886-MS)
4. Carr, T. R., Thomas H. Wilson, T. H., Payam Kavousi, P., Amini, S., Sharma, S., Hewitt, J., Costello, I., Carney, B.J., Jordon, E., Yates, M., MacPhail, K., Uschner, N., Thomas, M., Akin, S., Magbagbeola, O., Morales, A., Johansen, A., Hogarth, L., Anifowoshe, O., Naseem, K., Hammack, R., Kumar, A., Zorn, E., Vagnetti, R. and Dustin Crandall, D., 2017, Insights from the Marcellus Shale Energy and Environment Laboratory (MSEEL), Proceedings, Unconventional Resources Technology Conference (URTEC) DOI [10.15530-urtec-2017-2670437](https://doi.org/10.15530-urtec-2017-2670437), p. 1130–1142. <https://library.seg.org/doi/abs/10.15530/urtec-2017-2670437>
5. Carnahan, B.D., Clanton, R.W., Koehler, K.D., Harkins, G.O. and Williams, G.R., 1999, Fiber optic temperature monitoring technology: In SPE Western Regional Meeting. *Society of Petroleum Engineers*, SPE 54599. doi: [10.2118/54599-MS](https://doi.org/10.2118/54599-MS)
6. Cengel, Y.A. and Boles, M.A., 2002, *Thermodynamics: an engineering approach: Sea, 1000*, p.8862.

7. Deighton, I., Tibocho, E. and TGS, P.D., 2014, MaxG Basin Temperature Modelling Using Bottom Hole Temperature Datasets: In SPE/AAPG/SEG Unconventional Resources Technology Conference. doi: [10.15530/URTEC-2014-1920520](https://doi.org/10.15530/URTEC-2014-1920520)
Fridleifsson, I.B., Bertani, R., Huenges, E., Lund, J.W., Ragnarsson, A., and Rybach, L., 2008, The possible role and contribution of geothermal energy to the mitigation of climate change, in Hohmeyer, O., and Trittin, T., eds., 2008, IPCC scoping meeting on renewable energy sources: Proceedings, Intergovernmental Panel on Climate Change, Lubeck, Germany: World Meteorological Organization, United Nations Environmental Programme, p. 59–80
8. Frone, Z.S., Blackwell, D.D., Richards, M.C. and Hornbach, M.J., 2015, Heat flow and thermal modeling of the Appalachian Basin, West Virginia: *Geosphere*, **11**(5), pp.1279–1290. doi: [10.1130/GES01155.1](https://doi.org/10.1130/GES01155.1)
9. Ghahfarokhi, P.K., Carr, T., Song, L., Shukla, P. and Pankaj, P., 2018, Seismic Attributes Application for the Distributed Acoustic Sensing Data for the Marcellus Shale: New Insights to Cross-Stage Flow Communication: In SPE Hydraulic Fracturing Technology Conference and Exhibition. *Society of Petroleum Engineers*, SPE 189888. doi: [10.2118/189888-MS](https://doi.org/10.2118/189888-MS)
10. Gonzalez, S., Al Rashidi, H., Pandey, D.C., Al-Mula, Y., Safar, A., Al-Kandari, J., Abdalla, W.A., Gorgi, S. and Patel, D., 2018, Real-Time Fiber-Optics Monitoring of Steam Injection in Unconsolidated High Viscous Formation: In SPE EOR Conference at Oil and Gas West Asia. *Society of Petroleum Engineers*, SPE 190362. doi: [10.2118/190362-MS](https://doi.org/10.2118/190362-MS)
11. Johnson, D.O., Sierra, J.R., Kaura, J.D. and Gualtieri, D., 2006, Successful flow profiling of gas wells using distributed temperature sensing data: In SPE Annual Technical Conference and Exhibition. *Society of Petroleum Engineers*, SPE 103097. doi: [10.2118/103097-MS](https://doi.org/10.2118/103097-MS)
12. Kabir, C.S., Izgec, B., Hasan, A.R., Wang, X. and Lee, J., 2008, Real-time estimation of total flow rate and flow profiling in dts-instrumented wells: In International Petroleum Technology Conference. *International Petroleum Technology Conference*. doi: [10.2523/IPTC-12343-MS](https://doi.org/10.2523/IPTC-12343-MS)
13. Karaman, O.S., Kutlik, R.L. and Kluth, E.L., 1996, A field trial to test fiber optic sensors for downhole temperature and pressure measurements, West Coalinga field, California: In SPE Western Regional Meeting. *Society of Petroleum Engineers*, SPE 35685. doi: [10.2118/35685-MS](https://doi.org/10.2118/35685-MS)
14. Kavousi, P., Carr, T. R., Wilson, T., Amini, S., Wilson, C., Thomas, M., MacPhail, K., Crandall, D., Carney, B.J., Costello, I., and Hewitt J., 2017, Correlating distributed acoustic sensing (DAS) to natural fracture intensity for the Marcellus Shale. *SEG Technical Program Expanded Abstracts 2017*: pp. 5386–5390. <https://doi.org/10.1190/segam2017-17675576.1>
15. Lanier, G.H., Brown, G. and Adams, L., 2003, Brunei Field Trial of a Fibre Optic Distributed Temperature Sensor (DTS) System in a 1,000 m Open Hole Horizontal Oil Producer: In SPE Annual Technical Conference and Exhibition. *Society of Petroleum Engineers*, SPE 84324. doi: [10.2118/84324-MS](https://doi.org/10.2118/84324-MS)
16. Mishra, A., Al Gabani, S.H. and Jumaa Al Hosany, A., 2017, Pipeline Leakage Detection Using Fiber Optics Distributed Temperature Sensing DTS: In SPE Abu Dhabi International Petroleum Exhibition & Conference. *Society of Petroleum Engineers*, SPE 188407. doi: [10.2118/188407-MS](https://doi.org/10.2118/188407-MS)
17. Nath, D.K., Sugianto, R. and Finley, D., 2005, Fiber-optic distributed temperature sensing technology used for reservoir monitoring in an Indonesia steam flood: In SPE International Thermal Operations and Heavy Oil Symposium. *Society of Petroleum Engineers*, SPE 97912. doi: [10.2118/97912-MS](https://doi.org/10.2118/97912-MS)
18. Nath, D.K., Finley, D.B. and Kaura, J.D., 2006, Real-Time Fiber-Optic Distributed Temperature Sensing (DTS)-New Applications in the Oilfield: In SPE Annual Technical Conference and Exhibition. *Society of Petroleum Engineers*, SPE 103069. doi: [10.2118/103069-MS](https://doi.org/10.2118/103069-MS)

19. Ouyang, L.B. and Belanger, D., 2004, Flow Profiling via Distributed Temperature Sensor (DTS) System-Expectation and Reality: In SPE Annual Technical Conference and Exhibition. *Society of Petroleum Engineers*, SPED 90541 doi: [10.2118/90541-MS](https://doi.org/10.2118/90541-MS)
20. Peck, D. and Seebacher, P., 2000, Distributed Temperature Sensing using Fibre-Optics (DTS Systems): Presented to Electricity Engineers's Association Annual Conference, Auckland, New Zealand.
21. Pinto, M.C., Karale, C. and Das, P., 2013, A simple and reliable approach for the estimation of the Joule-Thomson coefficient of reservoir gas at bottomhole conditions: *SPE Journal*, **18**(05), pp.960–968, SPE 158116. doi: [10.2118/158116-PA](https://doi.org/10.2118/158116-PA)
22. Roy, B.N., 2002, *Fundamentals of classical and statistical thermodynamics*: John Wiley & Sons.
23. Saputelli, L., Mendoza, H., Finol, J., Rojas, L., Lopez, E., Bravo, H. and Buitriago, S., 1999, Monitoring steamflood performance through fiber optic temperature sensing: In International Thermal Operations/Heavy Oil Symposium. *Society of Petroleum Engineers*, SPE 54104. doi: [10.2118/54104-MS](https://doi.org/10.2118/54104-MS)
24. Smolen, J.J. and van der Spek, A., 2003, *Distributed Temperature Sensing: A primer for Oil and Gas Production*. Shell.
25. Tolan, M., Boyle, M. and Williams, G., 2001, The use of fiber-optic distributed temperature sensing and remote hydraulically operated interval control valves for the management of water production in the Douglas field: In SPE Annual Technical Conference and Exhibition. *Society of Petroleum Engineers*, SPE 71676. doi: [10.2118/71676-MS](https://doi.org/10.2118/71676-MS)
26. Walker, I. and Carr, D., 2003, Fibre Optic Leak Detection: In Offshore Technology Conference. Offshore Technology Conference. doi: [10.4043/15360-MS](https://doi.org/10.4043/15360-MS)
27. Wang, X., Lee, J., Thigpen, B., Vachon, G.P., Poland, S.H. and Norton, D., 2008, Modeling flow profile using distributed temperature sensor (DTS) system: In Intelligent Energy Conference and Exhibition. *Society of Petroleum Engineers*, SPE 111790. doi: [10.2118/111790-MS](https://doi.org/10.2118/111790-MS)
28. Wang, Z., 2012, *The uses of distributed temperature survey (DTS) data (Doctoral dissertation, Stanford University)*.
29. Wheaton, B., Haustveit, K., Deeg, W., Miskimins, J. and Barree, R., 2016, A case study of completion effectiveness in the eagle ford shale using DAS/DTS observations and hydraulic fracture modeling: In SPE Hydraulic Fracturing Technology Conference. *Society of Petroleum Engineers*, SPE 179149. doi: [10.2118/179149-MS](https://doi.org/10.2118/179149-MS)